Turbulent Power Spectrum of the Interstellar Medium
PH354 Computational Physics Project

Shashank Dattathri
#13799
UG Fourth Year

1 Introduction

The interstellar medium (ISM) is studied by performing astronomical surveys at different frequencies, angular scales, and portions of the sky. These surveys record atomic, molecular, and dust emission spectra. A powerful method to study these emission spectra is through power spectrum analysis, which can reveal much about the dynamical and morphological properties of the ISM.

Data from astronomical surveys is usually released as FITS (flexible image transport system) files. The observables (brightness temperature, column density, etc) are recorded as a function of the independent variables. As we can only see a 2D projection of the sky, the x and y axes are usually position coordinates (galactic latitude and longitude, right accession and declination, etc). The observable is recorded for each position, which is commonly called an image. The third axis, if present, is typically the line of sight velocity (v_{lsr}) which is measured by the Doppler effect. This will constitute a PPV (position-position-velocity) data cube.

In this project, I perform power spectrum analysis with astronomical data of dust grain emission, neutral hydrogen emission, and CO molecular emission in the ISM. I record the power law indices for the various data sets and ISM phases. This method is then extended to calculate some basic three-dimensional properties of the astronomical body.

This report is organized as follows. In section 2, I present the basic theory of power spectrum calculations and how it is implemented in my code. I then implement it on two data sets: the Planck survey and the WISE survey, both of which measure dust grain emission in the ISM. In section 3, I analyze the turbulent power spectrum of the H1 emission of the multiphase ISM, and record the power law index over the different phases. In section 4, I extend this 2D analysis to calculate the 3D solenoidal fraction of the Orion B molecular cloud. I conclude in section 5.

2 Calculation of Power Spectrum

The power spectrum of an image is obtained by the following method. The brightness temperature T_B as a function of the two axes (which we will call x and y) is given in the form of a 2D array. If the original data is in the form of a PPV cube, the 2D image is formed by either integrating over the velocity axis or by taking a slice of the data cube at a particular velocity. So, we are left with a 2D array $T_B(x, y)$.
The average brightness temperature $\langle T_B \rangle$ of the image is calculated. This allows us to define

$$\theta_B(x, y) = T_B(x, y) - \langle T_B \rangle \tag{1}$$

which is the temperature fluctuation from the mean value.
The **autocorrelation** of a function $f(x)$ is defined as:

$$A_{ff}(\delta x) = \int_{-\infty}^{\infty} f(x) f(x + \delta x) dx \tag{2}$$

Since $\theta_B(x, y)$ is a function of two variables, the autocorrelation function $A(x, y)$ will be a 2D array.

$$A(\delta \mathbf{r}) = \int \int \theta_B(\mathbf{r}) \theta_B(\mathbf{r} + \delta \mathbf{r}) d^2\mathbf{r} \tag{3}$$

where $\mathbf{r} = \mathbf{x} + \mathbf{y}$.
The power spectral density of T_B is defined as the Fourier transform of the autocorrelation function. For our 2D case, we have

$$\mathcal{F}(k_x, k_y) = \int_{-\infty}^{\infty} \int_{-\infty}^{\infty} A(x, y) e^{-2\pi i (k_x x + k_y y)} dx\ dy \tag{4}$$

Note that strictly speaking, a Fourier transform in spherical coordinates should be used. However, since the image is only a small fraction of the total sky, it can be approximated as rectangular.
In general, $\mathcal{F}(k_x, k_y)$ is a complex value, and the power spectrum $P(k_x, k_y)$ is the absolute value of $\mathcal{F}(k_x, k_y)$.
Proceeding further, we assume isotropy in space: $P(k_x, k_y) = P(k)$ where $k = \sqrt{k_x^2 + k_y^2}$. This allows us to transform the 2D power

spectrum into 1D by averaging in the azimuthal direction.

The power spectrum is computed in my code as follows:

- The value of T_B as a function of galactic longitude and latitude is stored in an n x n array. The FITS file is read using the **astropy** package. The T_B data is smoothed along the velocity axis using a boxcar function of odd width.
- The value of $\langle T_B \rangle$ is calculated, and used to form the 2D array θ_B. As discrete Fourier transforms require the data to be periodic, θ_B is multiplied by a window function: $\theta_B[i][j] \leftarrow \theta_B[i][j] \sin(\pi i/n) \sin(\pi j/n)$.
- The autocorrelation function $A(x, y)$ is calculated from θ_B by using the function **correlate2d()** from the package **scipy.signal**. A normalizing constant of $1/n^4$ is multiplied.
- The 2D Fourier transform of $A(x, y)$ is performed using the function **fft2()** from the package **scipy.fftpack**. The zero-wavenumber component is shifted to the center of the array by using the function **fftshift()**. The power spectrum $P(k_x, k_y)$ is obtained by taking the absolute value.
- The power spectrum is azimuthally averaged using the function **aave()**. This function takes the 2D power spectrum $P(k_x, k_y)$ and returns a 1D array $P(k)$ by sorting $P(k_x, k_y)$ into bins of similar k values.
- A plot of $P(k)$ vs k is used to fit the curve to the relation $P(k) = Ak^{\beta}$. Instead of fitting directly, it is convenient to fit a straight line to $\log(P(k))$ vs $\log(k)$.

I now apply this theory and use my code to calculate the power spectrum of dust grain emission in the ISM. I perform the analysis with two data sets. The Planck survey is an all-sky survey of thermal dust emission at 857 GHz (350 μm). The data is stored in the form of a HEALPix FITS file, which I analyzed using the **astropy_healpix** package. The column density is shown in figure 1 for a 15° x 15° image centered at $(l, b) = (198°, 32°)$. I perform the power spectrum analyis for this image, using the steps outlined above.

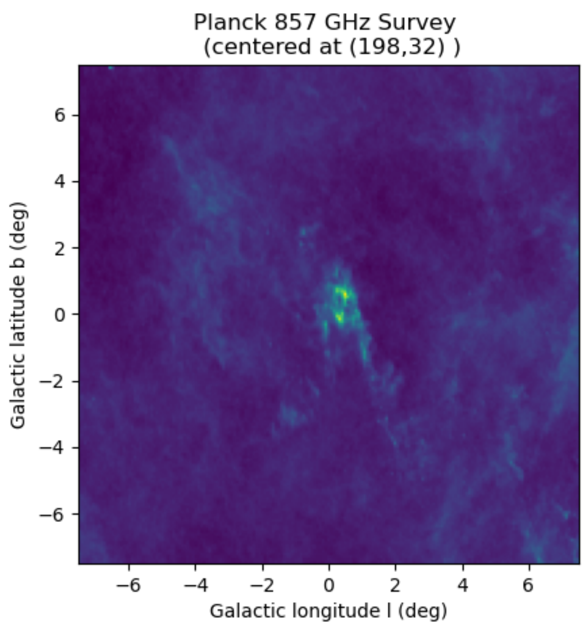

Figure 1: Density map for a 15° x 15° image centered at $(l, b) = (198°, 32°)$, from the Planck survey.

The power spectrum is shown in figure 2. The value of $\beta = -2.88 \pm 0.04$ that I obtain is in reasonable agreement with the value of $\beta = -2.7 \pm 0.1$ from [3]. The slight discrepancy is probably because they use specialized software to filter out noise and remove all background stars and galaxies before performing the analysis.

The WISE 12 μm map [4] is an all-sky survey which primarily observes the emission from the smallest dust grains. I perform the power spectrum analysis centered for a 4.7° x 4.7° image centered at the same point. The result is shown in figure 3. I obtain a value of $\beta = -2.84 \pm 0.09$, which is in good agreement with the published value of $\beta = -2.9 \pm 0.1$ [3].

3 Turbulent Power Spectrum of Multiphase ISM

The previous section was pertaining to the power spectrum of continuum dust emission. Another important method to survey the ISM is study of the neutral hydrogen (H1) 21 cm line. The Leiden/Argentine/Bonn (LAB) survey is a sensitive survey of the H1 emission in the Milky Way [5]. The data is stored in the form of a FITS PPV data cube. This allows us to distinguish between the different phases of the ISM, and to analyze how the power spectrum index changes across phases.
In this study, a region centered around $(l, b) = (198°, 32°)$ is selected. I plot the spatially averaged brightness temperature as a function of v_{lsr} for various image dimensions (deg x deg) in figure 4. Note that T_B is not symmetric in v_{lsr}.

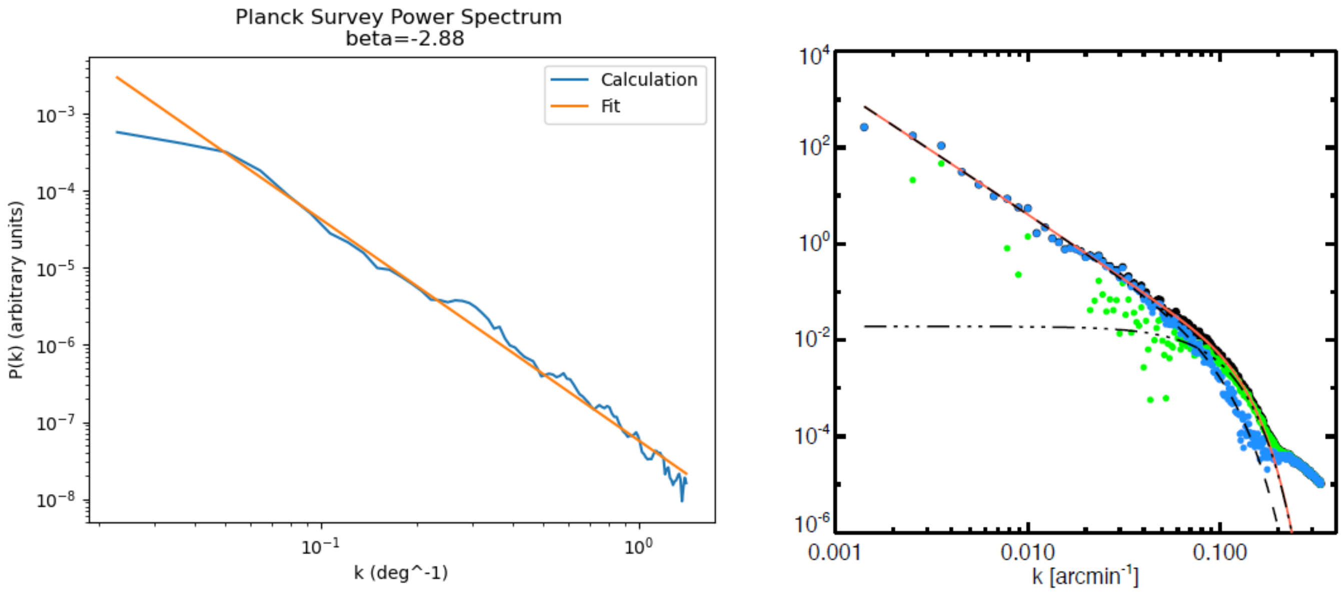

Figure 2: Left: power spectrum of the Planck survey at $(l, b) = (198°, 32°)$ in arbitrary units. Right: the corresponding figure from [3].

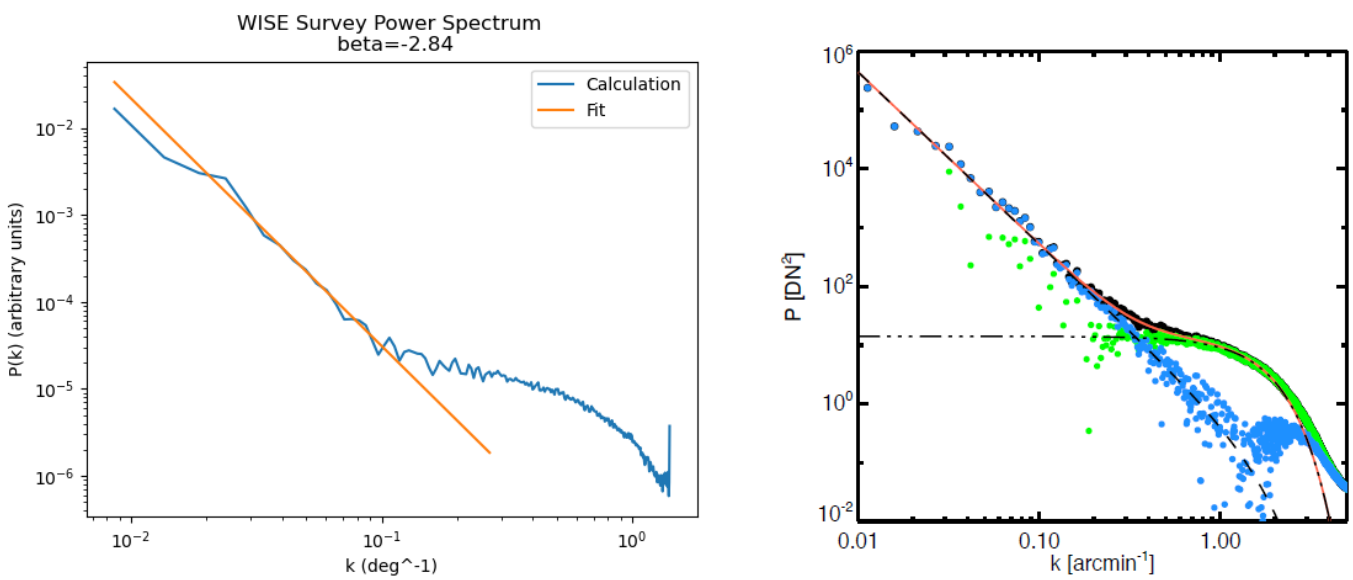

Figure 3: Left: power spectrum of the WISE survey at $(l, b) = (198°, 32°)$ in arbitrary units. Right: the corresponding figure from [3].

Studies of the ISM have shown the existence of three distinct phases: the warm neutral medium (WNM), cold neutral medium (CNM), and the intermediate velocity component (IVC). The various components dominate in different velocity ranges: the CNM in -4 to +15 km/s, IVC in -30 to -15 km/s, and WNM in -14 to -5 km/s and 15+ km/s. Using the function **optimise()** from the **scipy** package, I fit the 5° x 5° image to a two-component Gaussian function. The fit reveals that at small velocity magnitudes, the WNM dominates the positive velocity range, while the CNM dominates the negative velocity range.

Our goal is to plot the value of β from the fit $P(k) = Ak^{\beta}$ for different values of v_{lsr}. An image size of 20° x 20° centered at $(l, b) = (198°, 32°)$ is chosen. The method for this is as follows:

- The PPV data cube is inputted and smoothed along the velocity axis using a boxcar function of odd width. Boxcar smoothing of width w replaces the field value at velocity v by averaging the values from $v - w/2$ to $v + w/2$ along the velocity axis. The value of T_B as a function of galactic longitude and latitude is stored in an n x n array.
- The power spectrum is calculated and azimuthally averaged using the same steps as the previous section.

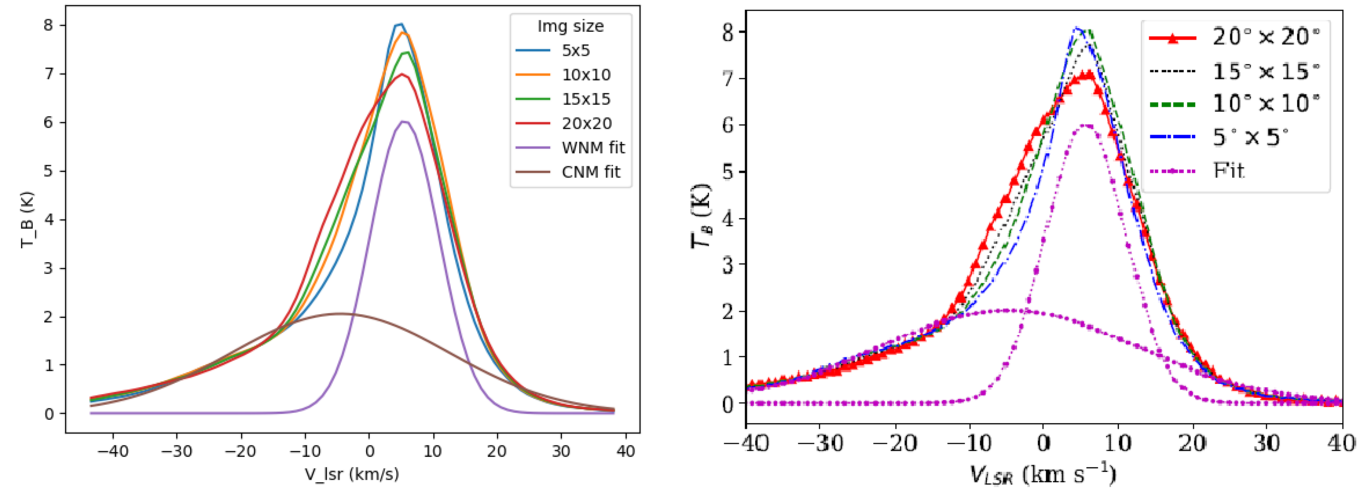

Figure 4: Left: spatially averaged T_B as a function of v_{lsr} for various image sizes, along with a two-component Gaussian fit for the 5° x 5° image. Right: the corresponding plot from [1].

- The power spectrum is fit to $P(k) = Ak^{\beta}$ for a selected range of k. I chose the k range as 0.3-0.9 because the power spectrum deviates from a simple power law at both small and large k values.
- The value of the power law index β and its error are plotted as a function of v_{lsr}.

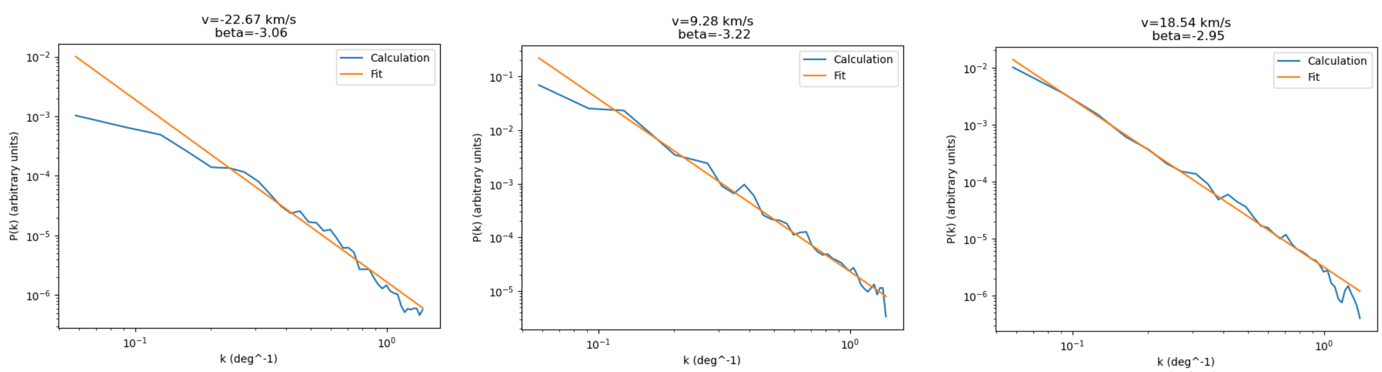

Figure 5: The azimuthal averaged power spectrum for different values of v_{lsr}.

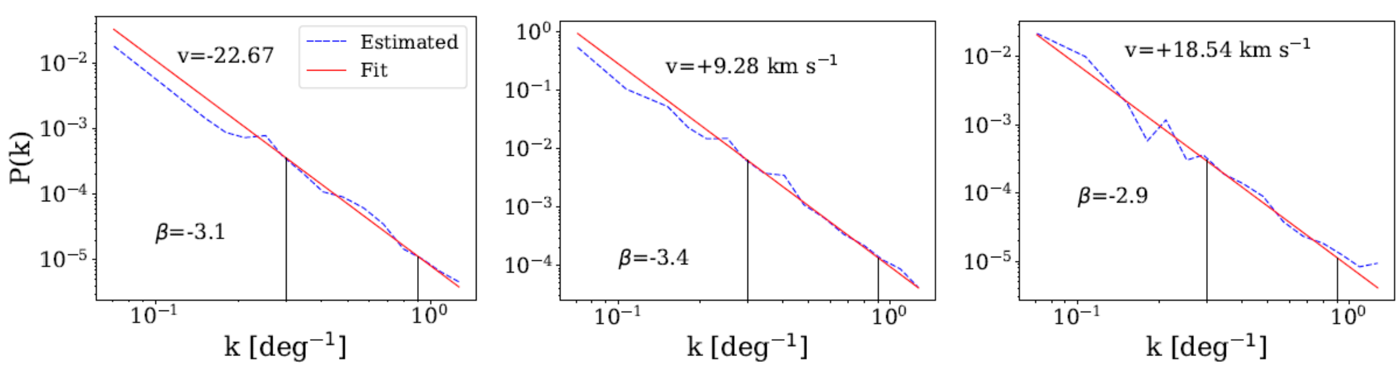

Figure 6: The corresponding figures from [1].

In figure 7, I plot β vs v_{lsr}, along with the median values for each of the phases. We can clearly see that the power law index changes as we go from one phase to the next. The results are tabulated in table 1.

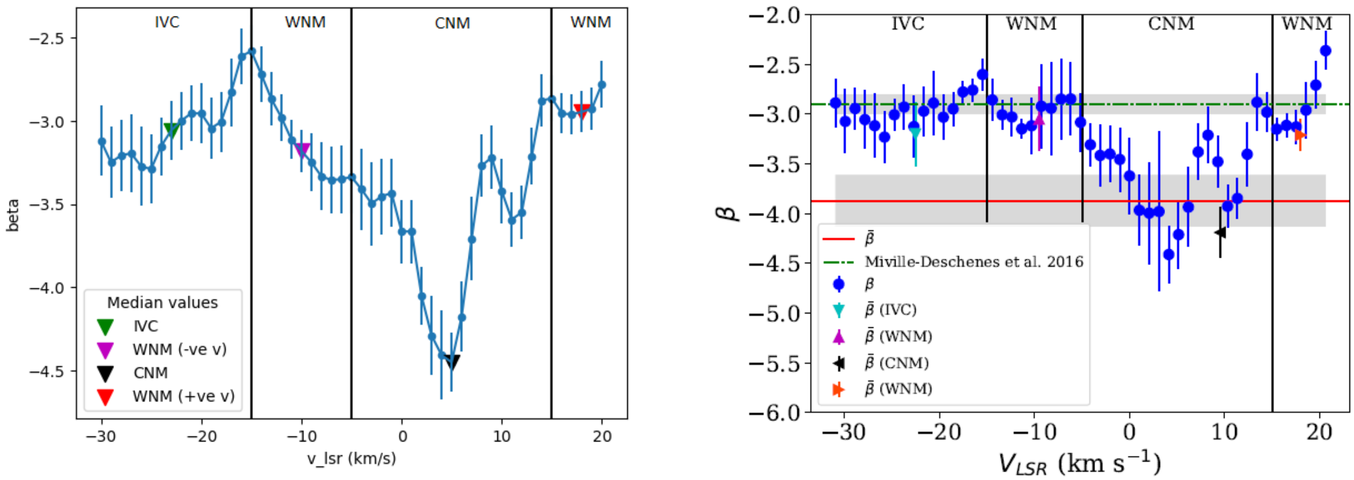

Figure 7: Left: β as a function of v_{lsr}. Right: the corresponding figure from [1].

Table 1: Results of β vs v_{lsr}

	IVC	**WNM (-ve v)**	**CNM**	**WNM (+ve)**	**Overall**
Median	-3.06	-3.18	-4.40	-2.95	-3.34
T_B **wtd. mean**	-3.02	-3.17	-3.70	-2.95	-3.48

Finally, we have to confirm that the observed power spectrum is produced by density fluctuations and not velocity fluctuations. I tabulate the value of β for $v_{lsr} = 9.28\ km/s$ for different widths of the boxcar smoothing function in table 2.

Table 2: Results of β vs boxcar width

Width	1	3	5	7	9	11	13
β	-3.22	-3.29	-3.43	-3.61	-3.79	-3.92	-3.97

We see that the power law index is a weak function of the boxcar width, so the fluctuations are dominated by density fluctuations and not velocity fluctuations. However, the weak dependence of β on the width indicate that the velocity fluctuations also may contribute to the power spectrum. In order to investigate this, I require data with a higher resolution in the velocity axis.

4 Three Dimensional Modeling

Since information from surveys is restricted to a projection of a field in two spatial dimensions, only limited information about the three-dimensional properties can be obtained. One important quantity in 3D turbulent motion is the solenoidal fraction, defined as

$$R = \sigma^2_{p_\perp}/\sigma^2_p \tag{5}$$

i.e. the ratio of the transverse (solenoidal) momentum variance to the total momentum variance. A lower value of R implies more momentum is in the compressive modes, while leads to greater star formation. A higher value implies more momentum in the solenoidal modes, leading to large-scale ordered rotation. Equipartition between the modes gives a solenoidal fraction of 2/3.
I follow the calculations from [6] and [7]. I use the $^{13}CO(J = 1 \to 0)$ emission line data from the IRAM-30 m telescope, surveying the Orion B molecular cloud. The original data is in the form of a PPV data cube, recording the column density (or equivalently, brightness temperature) along the three axis. The relevant quantities of interest are:

$$W_0 = \int I(v)dv \qquad W_1 = \int vI(v)dv \qquad W_2 = \int v^2 I(v)dv \tag{6}$$

which are the first, second, and third moments of the momentum field. The full PPV data cube is not yet available for public download. However, the FITS images of W_0, W_1, W_2 are available, which is what I start with.

The 2D power spectra $P_0(k_x, k_y)$ and $P_1(k_x, k_y)$ are calculated from W_0 and W_1. The quantities $f_0(k)$ and $f_1(k)$ are calculated as:

$$f_0(k) = \frac{1}{2\pi k}\int P_0(k,\phi)d\phi \qquad f_1(k) = \frac{1}{2\pi k}\int P_1(k,\phi)d\phi \tag{7}$$

which are just the azimuthal averages of the power spectra, divided by k. In my calculations, these quantities are calculated by a sum rather than an integral.
From this, other relevant factors are calculated:

$$A = \frac{\left(\sum_{k_x}\sum_{k_y}\sum_{k_z} f_0(k)\right) - f_0(0)}{\left(\sum_{k_x}\sum_{k_y} f_0(k)\right) - f_0(0)} \tag{8}$$

$$B = \frac{\left(\sum_{k_x}\sum_{k_y}\sum_{k_z} f_1(k)\frac{k_x^2+k_y^2}{k^2}\right) - f_1(0)}{\left(\sum_{k_x}\sum_{k_y} f_1(k)\right) - f_1(0)} \tag{9}$$

$$g_{12} = \frac{\langle\rho^2 v^2\rangle/\langle\rho^2\rangle}{\langle\rho v^2\rangle/\langle\rho\rangle} \tag{10}$$

where $\langle ... \rangle$ denotes spatial average. The solenoidal fraction R is calculated as

$$R = \left[\frac{\langle W_1^2\rangle}{\langle W_0^2\rangle}\right]\left[\frac{\langle W_0^2\rangle/\langle W_0\rangle^2}{1 + A(\langle W_0^2\rangle/\langle W_0\rangle^2 - 1)}\right]\left[g_{12}\frac{\langle W_2\rangle}{\langle W_0\rangle}\right]^{-1} B \tag{11}$$

In my code, I perform the calculations as follows.

- The 2D power spectra of W_0 and W_1 are calculated with the same methods as earlier sections.
- f_0 and f_1 are calculated using a modified version of the azimuthal averaging code.
- The quantities A, B, and g_{12} are calculated via the above formulae. This allows us to calculate R. Note that I use the original data without multiplying with a window function to find spatial averages.

From power spectrum analysis, I obtain a power law index of $\beta = -3.09 \pm 0.05$ and $\beta = -2.78 \pm 0.06$ for the power spectra of W_0 and W_1 respectively. This is in reasonable agreement with the results of [7], who obtained $\beta = -2.83 \pm 0.02$ and $\beta = -2.50 \pm 0.07$ respectively.
These calculations result in a solenoidal fraction value of $R = 0.77 \pm 0.03$, which is in solid agreement with the published value of $R = 0.72 \pm 0.09$ [7]. The R value is higher than the equipartional value of 2/3, which implies that solenoidal motion dominates the compression motion. This is in agreement with observations that Orion B has a low star forming efficiency, as star formation requires high compressive turbulent motion.

5 Conclusion

- Data from astronomical surveys are stored in the form of FITS and HEALPix FITS files. These files can be accessed in python using the **astropy** package.
- The power spectrum of dust emission in the ISM follows a power law with index $\beta \approx -2.9$, and this result matches well with published values.
- The turbulent power spectrum in the multiphase ISM, which was studied using the H1 21 cm emission, does not follow a simple universal power law. The power index varies from $\beta \approx 3$ for the IVC, to $\beta \approx 3.2$ for the WNM, to $\beta \approx 4$ for the CNM. The power law index is largely independent of the width of the velocity channel boxcar smoothing function, which shows that the turbulent power spectrum is primarily due to density fluctuations and not velocity fluctuations.
- We can use a PPV data cube to construct information about the three dimensional properties of the ISM. The solenoidal fraction of Orion B is calculated to be $R = 0.77$, which points to solenoidal motion dominating the turbulence and a low star forming efficiency.

List of files/functions used:

- **azimuthal_average.py**: contains the function **aave()**, which takes the two dimensional k-space array and power spectrum array as inputs, and returns the k-bin values and the azimuthal averaged 1D power spectrum. This file is used in all the other power spectrum calculations, and is not a standalone program.
- **Planck.py**: produces the column density plot and power spectrum of the Planck survey. Running time: about 30 seconds.
- **WISE.py**: produces the column density plot and power spectrum of the WISE survey. Reduces the data by a factor rf in each axis before analysis by boxcar smoothing. Running time: about a minute for $rf = 20$, takes longer time for smaller values of rf.
- **TB_vs_vlsr.py**: produces a plot of spatially averaged T_B as a function of v_{lsr} for the LAB H1 data. Also fits the 5° x 5° image to a two component Gaussian fit. Running time: about a minute.

- **Col_density_plot.py**: produces a column density image of the LAB H1 data for different phases of the ISM (IVC, WNM -ve, CNM, WNM +ve, whole). I did not include these figures in the report due to lack of space, but they correspond to figure 5 of [1]. Running time: a few seconds.
- **Multiphase_ISM.py**: produces the power spectrum plot of the LAB H1 data at any given velocity, and the β vs v_{lsr} plot. The **power_spec()** function calculates the power spectrum at each v_{lsr}, and the **main()** function stores the power law index at each v_{lsr} and produces the final plot. Running time: about a minute.
- **Solenoidal_fraction.py**: calculates the solenoidal fraction of the Orion B cloud using the $^{13}CO(J = 1 \rightarrow 0)$ emission line data from the IRAM-30 m telescope. Contains the functions **power_spectrum()** which calculates the power spectrum of W_0 and W_1, and **constants()** and **g12()** calculates the values of A, B, and g_{12}. The value of R is calculated in the **main()** function. Running time: about a minute.
- **main.py**: runs each of the above six standalone programs one by one. Running time: a couple of minutes.

All the power spectrum calculations use **azimuthal_average.py**, but the other files run independently of each other. For example, to run **Multiphase_ISM.py**, just input **python .\Multiphase_ISM.py** in the terminal. Executing **main.py** runs each of the six standalone programs one by one.

References

[1] S. Choudhuri and N. Roy. MNRAS, 483, p. 3437-3443, 2019.

[2] Planck Collaboration et al. A&A, 571, A11, 2014.

[3] Miville-Deschênes, M.-A., Duc, P.-A., Marleau, F., et al. A & A, 593, A4, 2016.

[4] Meisner, A. M. & Finkbeiner, D. P. ApJ, 781, 5, 2014.

[5] Kalberla, P. M. W., Burton, W. B., Hartmann, D., et al. A & A, 440, 775, 2005.

[6] Brunt, C. M., & Federrath, C. 2014, MNRAS, 442, 1451

[7] Orkisz, Jan H. et al. A & A, 599, A99, 2017.